Control Engineering Practice 18 (2010) 396–407

Contents lists available at ScienceDirect

Control Engineering Practice

journal homepage: www.elsevier.com/locate/conengprac

Identification of electrically stimulated muscle models of stroke patients

Fengmin Le *, Ivan Markovsky, Christopher T. Freeman, Eric Rogers

Information: Signals, Images, Systems Research Group, School of Electronics and Computer Science, University of Southampton, Southampton SO17 1BJ, UK

ARTICLE INFO

Article history:
Received 7 July 2009
Accepted 12 December 2009
Available online 25 January 2010

Keywords:
System identification
Hammerstein system
Muscle models
Alternating least squares
Functional electrical stimulation

ABSTRACT

Despite significant recent interest in the identification of electrically stimulated muscle models, current methods are based on underlying models and identification techniques that make them unsuitable for use with subjects who have incomplete paralysis. One consequence of this is that very few model-based controllers have been used in clinical trials. Motivated by one case where a model-based controller has been applied to the upper limb of stroke patients, and the modelling limitations that were encountered, this paper first undertakes a review of existing modelling techniques with particular emphasis on their limitations. A Hammerstein structure, already known in this area, is then selected, and a suitable identification procedure and set of excitation inputs are developed to address these short-comings. The technique that is proposed to obtain the model parameters from measured data is a combination of two iterative schemes: the first of these has rapid convergence and is based on alternating least squares, and the second is a more complex method to further improve accuracy. Finally, experimental results are used to assess the efficacy of the overall approach.

1. Introduction

Of the 300,000 people living in the UK with moderate to severe disabilities as a result of a stroke (National Audit Office, 2005), almost 85% had an initial deficiency in the upper limb (Parker, Wade, & Langton-Hewer, 1986) and less than 50% have recovered useful upper limb function (Broeks, Lankhorst, Rumping, & Prevo, 1999; Parker et al., 1986). Similar demographics exist across the EU, and due to an aging population and better acute care, prevalence of stroke is likely to increase. There is a growing body of clinical evidence (de Kroon, van der Lee, Ijzerman, & Lankhorst, 2002), and theoretical support from neurophysiology (Burridge & Ladouceur, 2001) and motor learning research, to support the use of electrical stimulation (ES) to improve motor control. There is also evidence that functional recovery is enhanced when stimulation is applied coincidently with a patient's voluntary intention whilst performing a task (Rushton, 2003). The need to accurately apply ES to achieve a movement has motivated significant interest in the development and application of techniques that can control upper limb movement to a high level of precision.

A diverse range of model-based schemes have been proposed for movement control of paralysed subjects, and include multi-channel PID control of the wrist (Watanabe, Iibuchi, Kurosawa, & Hoshimiya, 2003), optimal (Hunt, Munih, & Donaldson, 1997), H_∞ (Hunt, Jaime, & Gollee, 2001), and fuzzy (Davoodi & Andrews, 1998) control of standing, sliding mode control of shank movement (Jezernik, Wassink, & Keller, 2004a) and data-driven control (Previdi, Schauer, Savaresi, & Hunt, 2004) of the knee joint. Artificial neural networks have been applied to both the upper (Lan, Feng, & Crago, 1994; Tresadern, Thies, Kenney, Howard, & Goulermas, 2006) and lower limbs (Graupe & Kordylewski, 1997) of paretic subjects, although disadvantages to this last approach have been reported (Braz, Smith, & Davis, 2006).

A very significant feature to emerge from the literature is that these advanced techniques have not transfered to clinical practice. Here the strategies adopted are either open-loop, or the stimulation is triggered using limb position or Electromyographic (EMG) signals to provide a measure of participant's intended movement (de Kroon et al., 2002, 2005; de Kroon & Ijzerman, 2008). Closed-loop control has been achieved using EMG (Thorsen, Spadone, & Ferrarin, 2001) but this has not been incorporated in model-based controllers since EMG does not directly relate to the force or torque generated by the muscle. In the few cases where model-based control approaches have been used clinically, they have enabled a far higher level of tracking accuracy.

A principal reason for the lack of model-based methods finding application in a programme of patient trials is the difficulty in obtaining reliable biomechanical models of hemiplegic subjects. In the clinical setting there is minimal set-up time, reduced control over environmental constraints and little possibility of repeating any one test in the programme of treatment undertaken and consequently controllers are required to perform to a minimum standard across a wide number of subjects and

* Corresponding author.
E-mail address: fl07r@ecs.soton.ac.uk (F. Le).

0967-0661/$ - see front matter © 2010 Elsevier Ltd. All rights reserved.
doi:10.1016/j.conengprac.2009.12.007

conditions. However, the underlying musculoskeletal system is highly sensitive to physiological conditions (such as skin impedance, temperature and moisture) and electrode placement, as well as time-varying effects such as spasticity and fatigue (Baker, McNeal, Benton, Bowman, & Waters, 1993).

Iterative Learning Control (ILC) is one model-based approach that has found clinical application, as part of a research programme that involved the development of a robotic workstation for use by stroke patients in order to regain voluntary control of their impaired arm (Freeman et al., 2009a). Here, ES is applied to generate torque about the elbow joint, and ILC is used to update the stimulation level to assist their completion of a planar reaching task. In particular, the patient's hand is strapped to the robot and they attempt to follow a point moving along an illuminated elliptical track. Fig. 1 shows a stroke participant using the robotic workstation during one of their eighteen treatment sessions, and shows the shoulder strapping used to prevent trunk movement which would reduce the effectiveness of treatment. The error between the angle of the forearm in the horizontal plane, $\vartheta(t)$, and the required angle, $\vartheta^*(t)$, is measured during the task, and, at its conclusion, the robot returns the arm to the starting position. Fig. 2 shows the control scheme block diagram, which consists of a feedback controller, a linearizing controller and an ILC feedforward controller. The former block, taken as a proportional plus derivative controller in the clinical tests, acts as a pre-stabilizer and provides satisfactory tracking during initial trials. During the arm resetting time at the end of trial k, the ILC controller uses a biomechanical model of the arm and muscle system, along with the previous tracking error, to produce the feedforward update signal $\psi_{k+1}(t)$ for application in the next trial (full details of the ILC algorithms applied appears in Freeman et al., 2009a). The overall performance is clearly dependent on the accuracy of the arm and muscle model, which comprises

- a stimulated muscle structure which accounts for the torque, $y(t)$, acting about the elbow generated in response to the applied ES, $u(t)$,
- a kinematic model which gives the component of this torque in the horizontal plane of movement, and
- a two-link system which provides the resulting angular movement, $\vartheta(t)$.

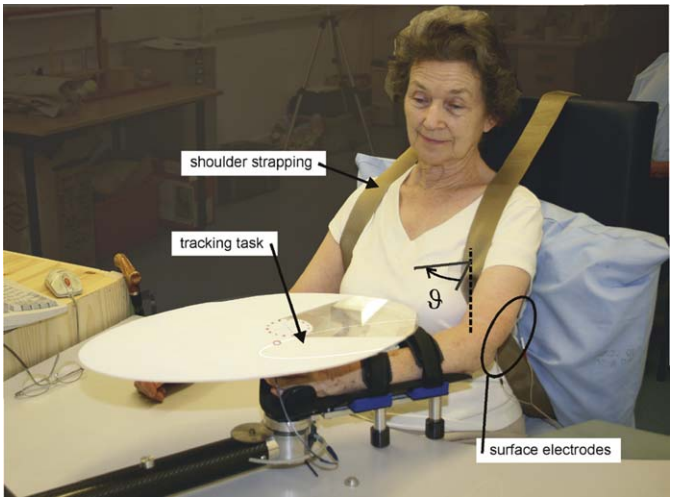

Fig. 1. A stroke participant using the robotic workstation.

The biomechanical model has been experimentally verified with both unimpaired subjects and stroke patients using a variety of functional parameter forms (Freeman et al., 2009b).

Although the model can predict arm movement resulting from applied ES with reasonable accuracy, experimental data confirms that the model of stimulated muscle adopted is not as accurately identified as the remaining components of the arm. The presence of such modelling inaccuracies necessitated use of relatively low ILC learning gains throughout the clinical trials, but the treatment still resulted in statistically significant improvement for participants across a number of outcome impairment measures (Hughes et al., 2009). The basic feasibility of the approach was therefore established, but the need for improved modelling of the patient's arm, and the muscle model, in particular, was also highlighted.

This paper first critically reviews the range of electrically-stimulated muscle models that have been proposed, and then develops a novel iterative identification method for use with stroke patients which addresses limitations in the existing approaches, relating not only to the component forms appearing in the model and the identification procedure applied, but to the type and duration of input signal, and the verification methods undertaken. Experimental tests are then performed to compare its performance to that of leading alternative methods.

2. Modelling of electrically stimulated muscle

The muscle models adopted in the wide range of model-based controllers that have been proposed for both the upper and lower limb also vary widely in structure. No explicit form of muscle model is used by Popovic and Popovic (1998), Crago, Nakai, and Chizeck (1991), and Chizeck, Lan, Palmieri, and Crago (1991) linear forms appear in Watanabe et al. (2003) and Hatwell, Oderkerk, Sacher, and Inbar (1991) and a general nonlinear form is assumed in Previdi et al. (2004). However, by far the most widely assumed structure is the Hill-type model (Hill, 1938), which describes the output force as the product of three independent experimentally measured factors: the force–length property, the force–velocity property and the nonlinear muscle activation dynamics under isometric conditions, termed simply activation dynamics (AD) of the stimulation input. The form of the first two is typically chosen to correspond with physiological observations (see, for example, Jezernik, Wassink, & Keller, 2004b; Lan, 2002; Riener & Fuhr, 1998), but they have also been combined in a more general functional form (Freeman et al., 2009b; Schauer et al., 2005). The activation dynamics are almost uniformly represented by a Hammerstein structure comprising a static nonlinearity in series with linear dynamics. These constitute an important component of the model since controlled motions are typically smooth and slow, so that the effects of inertia, velocity, and series elasticity are small and the isometric behaviour of muscle dominates. The nonlinearity has been

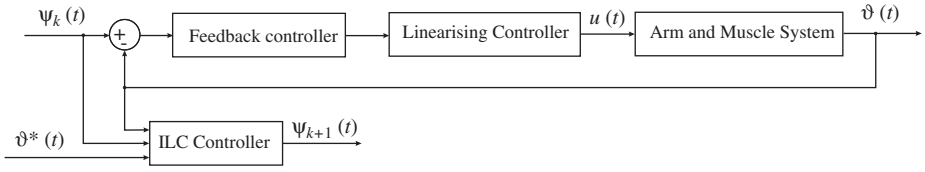

Fig. 2. Block diagram of ILC control scheme.

parametrized in a number of ways, taking the form of a simple gain with saturation (Ferrarin, Palazzo, Riener, & Quintern, 2001), a piecewise linear function (Hunt, Munih, Donaldson, & Barr, 1998; Lan, 2002) and a predefined functional form (Previdi & Carpanzano, 2003; Riener & Quintern, 1997). The linear dynamics have been assumed to be first order in Lan (2002), a series of two first order systems (Happee & der Helm, 1995; Jezernik et al., 2004a; Riener & Fuhr, 1998), critically damped second order (Baratta & Solomonow, 1990; Durfee & MacLean, 1989; Veltink, Chizeck, Crago, & El-Bialy, 1992) or second order with possible transport delay (Chizeck, Crago, & Kofman, 1988; Hunt et al., 1998).

The popularity of such a Hammerstein structure to represent the activation dynamics is due to correspondence with biophysics: the static nonlinearity, $f(u)$, represents the Isometric Recruitment Curve (IRC), which is the static gain relation between stimulus activation level, $u(t)$, and steady-state output torque, $w(t)$, when the muscle is held at a fixed length. The linear dynamics, $G(q)$, represents the muscle contraction dynamics, which combines with the IRC to give the overall torque generated, $y(t)$. These components are shown in Fig. 3. Identification of the activation dynamics is often accomplished using a pseudo-random binary sequence (PRBS) which enables the linear and nonlinear components to be separated (Bernotas, Crago, & Chizeck, 1986). The separation of components to facilitate identification has also been achieved through use of pulse and step signals (Durfee & MacLean, 1989; Munih et al., 2000).

Recent work has shown that Hill–Huxley models (see Bobet & Stein, 1998; Bobet, Gossen, & Stein, 2005; Ding, Wexler, & Binder-MacLeod, 2002) may be at least as accurate as a Hammerstein structure in representing the activation dynamics (Law & Shields, 2007). The drawback that their complexity undermines application to control has been countered by the proposal of a Hammerstein–Wiener structure (Bai, Cai, Dudley-Javorosk, & Shields, 2009), but as yet Hill–Huxley models have not been shown to extend to non-isometric conditions, and have not been used in controller derivation.

Due to its track record in the design and subsequent implementation of controllers, it is the Hammerstein structure that will be considered in this paper. As it stands, however, significant limitations exist in its application to upper limb stroke rehabilitation:

- ES has been applied to either *in vitro*, or paretic muscles in the vast majority of experimental verification tests. This effectively removes the possibility of an involuntary response to stimulation which may occur when applied to subjects with incomplete paralysis (such as stroke). As well as motivating the need for experimental validation on such subjects, this also means that the excitation inputs widely used to identify the Hammerstein structure (PRBS, white noise and pulses) are not appropriate as they would elicit an involuntary response from the subject.
- The absence of test results from subjects with incomplete paraplegia also means that physiologically based constraints on the form of the dynamics (such as the assumption of a critically damped system (Bernotas et al., 1986; Durfee & Palmer, 1994)) may not be justified.
- Almost all *in vivo* studies and control implementations have applied ES to the lower limb, even though upper limb functional tasks require finer control, and are more subject to adverse effects such as sliding electrodes and the activation of adjacent muscles during stimulation.

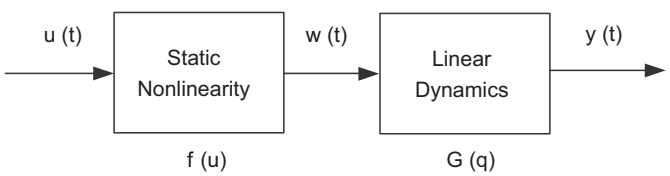

Fig. 3. Hammerstein structure representation of activation dynamics.

A novel identification scheme, and accompanying set of excitation inputs, will therefore be developed in this paper in order to address these drawbacks. Following the previous discussion, the necessary attributes are as follows:

- Since the excitation signal must be chosen from a physiological perspective, the identification scheme cannot use rapidly changing inputs and must be applicable to an arbitrary choice of signal.
- A general form of linear dynamics will be considered, represented in transfer-function form.
- The use of a smooth function with continuous derivatives is preferable to that of a piecewise linear function in the representation of the static nonlinearity.

The physical realization of the input is a more arbitrary consideration: the stimulus activation level, quantified by the number of muscle fibres activated, can be achieved by varying either the current or voltage amplitude, or the duration (width) of stimulus pulses. The latter method is preferable since it is easier to quantify and control, provides a more consistent response across subjects, requires a smaller charge per stimulus pulse, and allows for greater selectivity of recruitment than amplitude modulation (Crago, Peckham, & Thrope, 1980).

The modulation by temporal summation (stimulus period modulation, or, inversely, pulse frequency modulation), achieved by varying the time interval between the start of successive pulses, can be incorporated using a multiplicative function (Riener & Fuhr, 1998). It will not be used here, however, because: (i) the use of high frequencies (>50 Hz) has been shown in Baker et al. (1993) to increase muscle fatigue in stroke patients (frequencies up to 100 Hz are used in the frequency modulation method of Ding et al., 2002) and (ii) frequency modulation alone may not generate the range of torque needed to achieve the wide variety of functional tasks required by a stroke rehabilitation programme (Carroll, Triolo, Chizeck, Kobetic, & Marsolais, 1989).

Having established the model structure, the task of estimating the model parameters is now considered from a systems identification perspective. There are many methods applicable to Hammerstein models, and in general they can be classified into two categories: iterative and non-iterative methods, respectively. An example of the first class of methods was first introduced in Narendra and Gallman (1966), in which an iterative algorithm was proposed for the linear component, together with an output-error criterion minimization to yield the nonlinear part. However, this algorithm may not converge as illustrated by a counter-example (Stoica, 1981), where divergence occurred. Further work belonging to this category includes a relaxation iteration scheme (Zhu, 2000), and a separable least squares algorithm (Dempsey & Westwick, 2004; Westwick & Kearney, 2001). The implementation of the separable least squares optimization algorithm initially incorporated the use of a polynomial to represent the static nonlinearity (Westwick & Kearney, 2001). Cubic splines were subsequently adopted in order to overcome the problem that a high order polynomial is frequently required when describing hard linear constraints, and has problems associated with oscillatory behaviour (Dempsey & Westwick, 2004). Both the

methods of Westwick and Kearney (2001) and Dempsey and Westwick (2004) have been applied to a biological system (stretch reflex electromyogram) and produced a more accurate model than previous iterative identification approaches.

Turning to the non-iterative category, an equation-error parameter estimation method was reported in Chang and Luus (1971), an over-parametrization method in Boutayeb, Aubry, and Darouach (1996), an optimal two-stage algorithm in Bai (1998), which is based on recursive least squares and singular value decomposition, a blind approach in Bai (2002), and decoupling methods in Bai (1998), which separate the linear and nonlinear components and identify each block separately.

In this paper, an iterative technique will be applied since this generally leads to improved accuracy. Following the discussion above, the separable least squares method using cubic spline nonlinearities (Dempsey & Westwick, 2004) appears most appropriate based on its success in modelling stretch reflex dynamics. The approach involves dividing the parameters into the linear and nonlinear parts: the nonlinear parameters start from initial values and then have been updated on each iteration using the Levenberg–Marquardt algorithm to compute the step, and the linear parameters are then similarly updated by linear regression. However, this approach cannot be applied to the present problem since it relies on a finite impulse response representation of dynamics, rather than the infinite impulse transfer-function form that has been adopted in the vast majority of the Hammerstein structure applications to muscle modelling, and which also leads to reduced memory requirement and computational work load. Therefore, since Dempsey and Westwick (2004) is unsuitable, an iterative algorithm will be developed for identification of the form of Hammerstein structure stipulated, which uses a different projection approach to update the nonlinear parameters. The iterative algorithm will be developed in Section 4 and experimental results using a human subject will be presented in order to evaluate this method with respect to its convergence properties, identification and predictive abilities. To support the choice of approach taken, results in Le, Markovsky, Freeman, and Rogers (2009) show the approach developed in this paper leads to superior performance when compared with both the least squares method with polynomial nonlinearity (Westwick & Kearney, 2001), and the ramp deconvolution method (Durfee & MacLean, 1989) used in the ILC project described in Section 1.

3. Identification problem statement

Two discrete-time Hammerstein model structures will be considered and are shown in Fig. 4. The stimulation input u is first scaled by the static nonlinear function f and then passed to a linear time-invariant system described by a transfer-function $G(q)=B(q)/A(q)$. The internal signal w is not measurable and the noise v is zero mean and white.

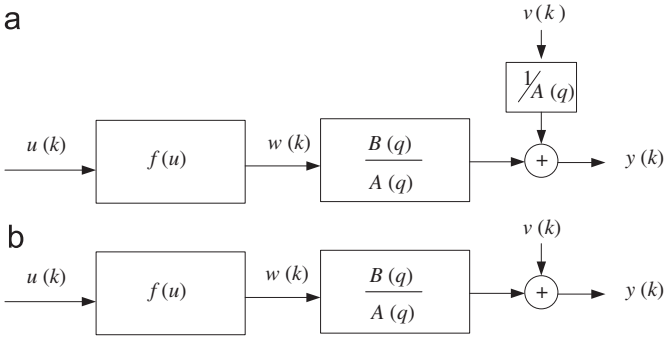

Fig. 4. Two discrete-time Hammerstein model structures: (a) ARX model and (b) OE model.

The linear system is represented by the transfer-function

$$G(q)=\frac{B(q)}{A(q)}=\frac{b_0q^{-d}+b_1q^{-(d+1)}+\cdots+b_nq^{-(n+d)}}{1+a_1q^{-1}+\cdots+a_lq^{-l}} \tag{1}$$

where q^{-1} is the delay operator and n, l and d are the number of zeros, poles and the time delay order, respectively. The parameters n, l and d are assumed to be known.

The nonlinear function $f(u)$ is represented by the cubic spline

$$f(u)=\sum_{i=1}^{m-2}\beta_i|u-u_{i+1}|^3+\beta_{m-1}+\beta_m u+\beta_{m+1}u^2+\beta_{m+2}u^3 \tag{2}$$

where $u_{\min}=u_1<u_2<u_3<\cdots<u_m=u_{\max}$ are the spline knots,

$$\theta_n=[\beta_1 \quad \beta_2 \quad \cdots \quad \beta_{m+2}]^T$$

are the parameters of the nonlinear block and

$$\theta_l=\begin{bmatrix}\theta_a\\ \theta_b\end{bmatrix}=[a_1 \quad \cdots \quad a_l \quad b_0 \quad b_1 \quad \cdots \quad b_n]^T \tag{3}$$

are the parameters of the linear block.

The difference between the two Hammerstein models lies in the form of the noise model. In Fig. 4(a) an Auto Regressive eXternal (ARX) model is used, in which the noise filter, $H=1/A(q)$, is coupled to the linear component of the plant model. In Fig. 4(b) an Output-Error (OE) model is used instead and in this case, the noise model is $H=1$.

The identification problem is now defined as follows: given collected input/output data

$$((u(1),y(1)),\ldots,(u(N),y(N)))$$

find a parameter vector

$$\theta=\begin{bmatrix}\theta_n\\ \theta_l\end{bmatrix}$$

that minimizes the cost function

$$\|v\|_2^2=\sum_{k=1}^{N}v^2(k) \tag{4}$$

where

$$\frac{1}{\hat{A}(q)}v=y-G(q,\hat{\theta}_l)f(u,\hat{\theta}_n)=y-\frac{\hat{B}(q)}{\hat{A}(q)}f(u,\hat{\theta}_n) \tag{5}$$

in the case of the ARX noise model and

$$v=y-G(q,\hat{\theta}_l)f(u,\hat{\theta}_n)=y-\frac{\hat{B}(q)}{\hat{A}(q)}f(u,\hat{\theta}_n) \tag{6}$$

in the case of the OE noise model.

4. Identification algorithm

4.1. Nonlinear parameter identification

Assume that an initial estimate of the linear parameter vector, $\hat{\theta}_l$, is available. Then the nonlinear parameters can be identified using the initial estimate of the linear parameter as follows.

- ARX model:
  Multiplying (5) by $\hat{A}(q)$ and substituting the resulting expression for v in (4) yields

$$\hat{\theta}_n=\underset{\theta_n}{\operatorname{argmin}}\|\hat{A}(q)y-\hat{B}(q)f(u,\theta_n)\|_2 \tag{7}$$

From (2), it follows that $f(u,\theta_n)$ is linear in θ_n, and hence

$$\begin{aligned}(\hat{B}(q)f(u,\theta_n))(k) &= \sum_{i=1}^{m-2}\beta_i\underbrace{(\hat{b}_0|u(k-d)-u_{i+1}|^3+\cdots+\hat{b}_n|u(k-d-n)-u_{i+1}|^3)}_{f_i(u(k),\hat{\theta}_b)}\\ &+\beta_{m-1}\underbrace{(\hat{b}_0+\cdots+\hat{b}_n)}_{f_{m-1}(u(k),\hat{\theta}_b)}+\beta_m\underbrace{(\hat{b}_0u(k-d)+\cdots+\hat{b}_nu(k-d-n))}_{f_m(u(k),\hat{\theta}_b)}\\ &+\beta_{m+1}\underbrace{(\hat{b}_0u(k-d)^2+\cdots+\hat{b}_nu(k-d-n)^2)}_{f_{m+1}(u(k),\hat{\theta}_b)}\\ &+\beta_{m+2}\underbrace{(\hat{b}_0u(k-d)^3+\cdots+\hat{b}_nu(k-d-n)^3)}_{f_{m+2}(u(k),\hat{\theta}_b)}\end{aligned} \tag{8}$$

Therefore, (7) can be rewritten as an ordinary least squares problem

$$\underset{\theta_n}{\operatorname{argmin}}\|Y_n(y,\hat{\theta}_a)-\Phi_n(u,\hat{\theta}_b)\theta_n\|_2 \tag{9}$$

where assuming that $l>n+d$,

$$Y_n(y,\hat{\theta}_a)=\begin{bmatrix} y(l+1)+\hat{a}_1y(l)+\cdots+\hat{a}_ly(1)\\ y(l+2)+\hat{a}_1y(l+1)+\cdots+\hat{a}_ly(2)\\ \vdots\\ y(N)+\hat{a}_1y(N-1)+\cdots+\hat{a}_ly(N-l)\end{bmatrix}$$

and

$$\Phi_n(u,\hat{\theta}_b)=\begin{bmatrix} f_1(u(l+1),\hat{\theta}_b) & \cdots & f_{m+2}(u(l+1),\hat{\theta}_b)\\ f_1(u(l+2),\hat{\theta}_b) & \cdots & f_{m+2}(u(l+2),\hat{\theta}_b)\\ \vdots & & \vdots\\ f_1(u(N),\hat{\theta}_b) & \cdots & f_{m+2}(u(N),\hat{\theta}_b)\end{bmatrix}$$

The solution of (7) now is

$$\hat{\theta}_n=(\Phi_n(u,\hat{\theta}_b)^T\Phi_n(u,\hat{\theta}_b))^{-1}\Phi_n(u,\hat{\theta}_b)^TY_n(y,\hat{\theta}_a)$$

- OE model

Let $\hat{y}$ be the output of $\hat{G}$ when the input is $f(u,\theta_n)$, i.e.,

$$\hat{y}(k)=\frac{\hat{B}(q)}{\hat{A}(q)}f(u,\theta_n) \tag{10}$$

Multiplying both sides of (10) by $\hat{A}(q)$, gives

$$\hat{A}(q)\hat{y}(k)=\hat{B}(q)f(u,\theta_n) \tag{11}$$

and expanding $\hat{B}(q)f(u(k),\theta_n)$ as in (8) yields the matrix equation

$$T(\hat{\theta}_a)\hat{Y}=\Phi_n(u,\hat{\theta}_b)\theta_n \tag{12}$$

where

$$T(\hat{\theta}_a)=\begin{bmatrix}\hat{a}_l & \cdots & \hat{a}_1 & 1 & 0 & \cdots & \cdots & 0\\ 0 & \hat{a}_l & \cdots & \hat{a}_1 & 1 & \cdots & \cdots & 0\\ \vdots & & & & & & & \vdots\\ 0 & \cdots & \cdots & 0 & \hat{a}_l & \cdots & \hat{a}_1 & 1\end{bmatrix}\quad\text{and}\quad\hat{Y}=\begin{bmatrix}\hat{y}(1)\\ \hat{y}(2)\\ \vdots\\ \hat{y}(N)\end{bmatrix}$$

However, $T(\hat{\theta}_a)$ is an $(N-l)\times N$ matrix, which implies that the solution for $\hat{Y}$ is not unique. The system theoretic interpretation of this linear algebra fact is that the output cannot be uniquely determined by the given model and input. Indeed, there are additional degrees of freedom in the choice of the *initial conditions*. In order to make the solution of problem (12) unique, zero initial conditions are assumed. This choice is justifiable in the context of the muscle identification problem because the experiment starts with the muscle "at rest". The choice of zero initial conditions amounts to extending the data by zeros in the past, which in turn means that the matrices $T(\hat{\theta}_a)$ and $\Phi_n(u,\hat{\theta}_b)$ are extended to comprise N columns, and then (12) becomes

$$T_{ext}(\hat{\theta}_a)\hat{Y}=\Phi_n(u_{ext},\hat{\theta}_b)\theta_n \tag{13}$$

with

$$T_{ext}(\hat{\theta}_a)=\begin{bmatrix}1 & 0 & \cdots & 0 & 0 & \cdots & \cdots & 0\\ \hat{a}_1 & 1 & 0 & 0 & 0 & \cdots & \cdots & 0\\ \vdots & \ddots & & & & & & \vdots\\ \hat{a}_l & \cdots & \hat{a}_1 & 1 & 0 & \cdots & \cdots & 0\\ 0 & \hat{a}_l & \cdots & \hat{a}_1 & 1 & \cdots & \cdots & 0\\ \vdots & & & & & & & \vdots\\ 0 & \cdots & \cdots & 0 & \hat{a}_l & \cdots & \hat{a}_1 & 1\end{bmatrix}$$

and

$$\Phi_n(u_{ext},\hat{\theta}_b)=\begin{bmatrix} f_1(u(1),\hat{\theta}_b) & \cdots & f_{m+2}(u(1),\hat{\theta}_b)\\ f_1(u(2),\hat{\theta}_b) & \cdots & f_{m+2}(u(2),\hat{\theta}_b)\\ \vdots & & \vdots\\ f_1(u(N),\hat{\theta}_b) & \cdots & f_{m+2}(u(N),\hat{\theta}_b)\end{bmatrix}$$

Consequently, from (13)

$$\hat{Y}=T_{ext}^{-1}(\hat{\theta}_a)\Phi_n(u_{ext},\hat{\theta}_b)\theta_n$$

and substituting this expression for $\hat{Y}$ in (6), the cost function (4) becomes

$$\hat{\theta}_n=\underset{\theta_n}{\operatorname{argmin}}\|Y-T_{ext}^{-1}(\hat{\theta}_a)\Phi_n(u_{ext},\hat{\theta}_b)\theta_n\|_2$$

which can be solved approximately in the least squares sense to obtain the estimate of the nonlinear parameter vector, $\hat{\theta}_n$

$$\begin{aligned}\hat{\theta}_n=&((T_{ext}^{-1}(\hat{\theta}_a)\Phi_n(u_{ext},\hat{\theta}_b))^TT_{ext}^{-1}(\hat{\theta}_a)\Phi_n(u_{ext},\hat{\theta}_b))^{-1}\\ &(T_{ext}^{-1}(\hat{\theta}_a)\Phi_n(u_{ext},\hat{\theta}_b))^TY\end{aligned}$$

4.2. Linear parameters identification

Given an estimate $\hat{\theta}_n$ for the nonlinear parameter vector θ_n, the cost function (4) can be minimized over the linear parameter vector θ_l. This subproblem is a linear least squares minimization in the ARX case but a difficult nonlinear least squares problem in the OE case.

- ARX model

The minimization problem in the case of an ARX model is

$$\hat{\theta}_l=\underset{\theta_l}{\operatorname{argmin}}\|A(q)y-B(q)f(u,\hat{\theta}_n)\|_2$$

or in matrix form

$$\underset{\theta_l}{\operatorname{argmin}}\|Y'-\Phi_l(u,y,\hat{\theta}_n)\theta_l\|_2 \tag{14}$$

where

$$Y'=[y(l+1)\quad y(l+2)\quad\cdots\quad y(N)]^T$$

and

$$\Phi_l(u,y,\hat{\theta}_n)=\begin{bmatrix} -y(l) & \cdots & -y(1) & f(u(l+1-d),\hat{\theta}_n) & \cdots & f(u(l+1-d-n),\hat{\theta}_n)\\ -y(l+1) & \cdots & -y(2) & f(u(l+2-d),\hat{\theta}_n) & \cdots & f(u(l+2-d-n),\hat{\theta}_n)\\ \vdots & & \vdots & \vdots & & \vdots\\ -y(N-1) & \cdots & -y(N-l) & f(u(N-d),\hat{\theta}_n) & \cdots & f(u(N-d-n),\hat{\theta}_n)\end{bmatrix}$$

Therefore, the solution of (14) is

$$\hat{\theta}_l=(\Phi_l(u,y,\hat{\theta}_n)^T\Phi_l(u,y,\hat{\theta}_n))^{-1}\Phi_l(u,y,\hat{\theta}_n)^TY'$$

- OE model

  Recall the partition (3) of the transfer-function linear parameters vector θ_l into parameter θ_a of the denominator A and parameter θ_b of the numerator B. Then the output error can be minimized analytically over θ_b, reducing the number of optimization variables for the minimization problem.

  For given θ_a, (11) can be rewritten in a matrix form similar to (13) as

$$T_{ext}(\hat{\theta}_a)\hat{Y} = \Phi'_l(u_{ext}, \hat{\theta}_n)\theta_b \tag{15}$$

  where

$$\Phi'_l(u_{ext}, \hat{\theta}_n) = \begin{bmatrix} f(u(1-d), \hat{\theta}_n) & \cdots & f(u(1-d-n), \hat{\theta}_n) \\ f(u(2-d), \hat{\theta}_n) & \cdots & f(u(2-d-n), \hat{\theta}_n) \\ \vdots & & \vdots \\ f(u(N-d), \hat{\theta}_n) & \cdots & f(u(N-d-n), \hat{\theta}_n) \end{bmatrix}$$

  so that

$$\hat{Y}(\theta_a, \theta_b) = T_{ext}^{-1}(\hat{\theta}_a)\Phi'_l(u_{ext}, \hat{\theta}_n)\theta_b$$

  Thus, for a given $\hat{\theta}_a$, the solution, $\hat{\theta}_b$, for θ_b is given by

$$\hat{\theta}_b = \underset{\theta_b}{\operatorname{argmin}} \|Y - \hat{Y}\|_2$$

$$= \underbrace{((T_{ext}^{-1}(\hat{\theta}_a)\Phi'_l(u_{ext}, \hat{\theta}_n))^T T_{ext}^{-1}(\hat{\theta}_a)\Phi'_l(u_{ext}, \hat{\theta}_n))^{-1}(T_{ext}^{-1}(\hat{\theta}_a)\Phi'_l(u_{ext}, \hat{\theta}_n))^T Y}_{g(\hat{\theta}_a)} \tag{16}$$

  The OE minimization problem has now been reduced to an unconstrained nonlinear least squares problem

$$\hat{\theta}_a = \underset{\theta_a}{\operatorname{argmin}} \|Y - \hat{Y}(\theta_a, g(\theta_a))\|_2$$

  with optimization variable θ_a only. Such a problem can be solved by standard local optimization methods, e.g., the Levenberg–Marquardt method (Marquardt, 1963).

  Imposing stability of the identified model is in general difficult. In the muscle identification context, however, a second order system has been assumed by many authors, and in this case it can be shown that the stability constraint reduces to the following bound constraints on the parameters

$$0 < \hat{a}_2 \leq 1 \quad \text{and} \quad -2 \leq \hat{a}_1 \leq 0$$

4.3. Iterative algorithms

For both model structures, the minimization over the θ_n and θ_l parameters can be executed iteratively, which leads to Algorithms 1 and 2.

Algorithm 1. Iterative Algorithm for Hammerstein system Identification with ARX model

Inputs: an initial value of the linear component, $\hat{\theta}_l^0$, an input/output data set $u(k)$, $y(k)$, $k = 1, 2, \ldots, N$, and a convergence tolerance ε.

$j = 0$

repeat

$j = j+1$

$\hat{\theta}_n^j = (\Phi_n(u, \hat{\theta}_b^{j-1})^T \Phi_n(u, \hat{\theta}_b^{j-1}))^{-1} \Phi_n(u, \hat{\theta}_b^{j-1})^T Y_n(y, \hat{\theta}_a^{j-1})$

$\hat{\theta}_l^j = (\Phi_l(u, y, \hat{\theta}_n^j)^T \Phi_l(u, y, \hat{\theta}_n^j))^{-1} \Phi_l(u, y, \hat{\theta}_n^j)^T Y'$

until $|V_N(\hat{\theta}_l^j, \hat{\theta}_n^j) - V_N(\hat{\theta}_l^{j-1}, \hat{\theta}_n^{j-1})| < \varepsilon$

Output: $\hat{\theta} = \begin{bmatrix} \hat{\theta}_n^j \\ \hat{\theta}_l^j \end{bmatrix}$

Algorithm 2. Iterative Algorithm for Hammerstein system Identification with OE model

Inputs: an initial value of the linear component, $\hat{\theta}_l^0$, an input/output data set $u(k)$, $y(k)$, $k = 1, 2, \ldots, N$, and a convergence tolerance ε.

$j = 0$

repeat

$j = j+1$

$\hat{\theta}_n^j = ((T_{ext}^{-1}(\hat{\theta}_a^{j-1})\Phi_n(u_{ext}, \hat{\theta}_b^{j-1}))^T T_{ext}^{-1}(\hat{\theta}_a^{j-1})\Phi_n(u_{ext}, \hat{\theta}_b^{j-1}))^{-1}$
$(T_{ext}^{-1}(\hat{\theta}_a^{j-1})\Phi_n(u_{ext}, \hat{\theta}_b^{j-1}))^T Y$

$\hat{\theta}_a^j = \operatorname{argmin}_{\theta_a} \|Y - \hat{Y}(\theta_a, g(\theta_a))\|_2$ where $g(\theta_a)$ is defined in (16) and $\hat{\theta}_b^j = g(\hat{\theta}_a^j)$

until $|V_N(\hat{\theta}_l^j, \hat{\theta}_n^j) - V_N(\hat{\theta}_l^{j-1}, \hat{\theta}_n^{j-1})| < \varepsilon$

Output: $\hat{\theta} = \begin{bmatrix} \hat{\theta}_n^j \\ \hat{\theta}_l^j \end{bmatrix}$

5. Experimental test design

The choice of a suitable experimental test procedure is a crucial step for any successful model identification. This is especially true in the present case since tests are not applied to a mechanical or physical process, but to a human being; care must be taken to avoid triggering involuntary reflex mechanisms, fatigue, inhibition due to subject discomfort (Burridge & Ladouceur, 2001) and to operate within physiological constraints and limitations. Whilst the experimental test procedure ensures that the maximum levels of stimulation are within suitable bounds, as discussed in more detail in Section 6.1 below, it is also necessary to ensure that motor units are recruited gradually rather than abruptly exciting a large number simultaneously (Baker et al., 1993). This clearly excludes rapidly increasing input signals with wide amplitude fluctuation, and instead necessitates a more slowly varying signal to ensure the rate of recruitment of nerve fibres is limited above the excitation threshold. The need for a limitation on rapidly decreasing signals is also necessary since the sudden reduction in stimulation is also associated with involuntary reflexes and patient discomfort (Baker et al., 1993). A more subject-specific concern is that it has also been observed that certain types of signal elicit a greater degree of involuntary response than others, despite possessing similar characteristics.

As previously stated, the majority of excitation signals that have been applied are only suitable to the *in vitro* or completely paralysed case. Most schemes use step, impulse, or PRBS signals, and of these, the latter is the most common and has the effect of switching the activation level between two levels at each stimulus instant so that the whole nonlinearity is not excited and the linear dynamics alone may be identified. Having done so, the nonlinearity is then determined in a straightforward manner using another excitation signal and identification. Comparative simplicity is therefore paid for by the need for two separate test procedures. The procedure developed in Section 4 does not rely on such an approach, and hence can be used with a single excitation signal of shorter overall duration. By estimating both model components simultaneously, the proposed identification procedure is faster and also reduces the potential occurrence of muscle fatigue and physiological changes in the patient.

The necessary excitation signal should contain sufficient dynamic variation and also assume multiple levels distributed over the full amplitude range. Many signals satisfy this requirement, for example, staircase signals, Pseudo-Random Multi-level

Sequences (PRMS), multiple sinusoids, white noise and Filtered Random Noise (FRN). It is from these classes of signal that suitable inputs will be sought, with parameter values chosen to balance the persistency of excitement, as quantified through Hankel matrix analysis, and the suitability for application to unparalysed muscle. Of special interest are PRMS and FRN signals since these have been used in the application of a controller for the lower limb (Schauer et al., 2005) and identification of an upper limb model (Freeman et al., 2009b), respectively.

The ramp deconvolution method involves a step input and a slow ramp signal, each of which only satisfies one of the above criteria, but it appears to be the most appropriate identification method of those that have been used to provide a model for use in a control scheme (Durfee & MacLean, 1989; Durfee & Palmer, 1994; Chizeck, Chang, & Stein, 1999; Bobet et al., 2005; Freeman et al., 2009a). Moreover, it has been applied with both stroke patients and unimpaired subjects with reasonable accuracy and therefore comprises a baseline for comparative analysis.

Based on the above discussion, four candidate tests are proposed for the identification of electrically stimulated muscle, and examples of the excitation inputs used in each are given in Fig. 5, where, as discussed in Section 2, it is the pulse duration which is selected as the controlled variable. Experimental test results are presented in Section 6, and identification, validation and cross-validation results are also provided in order to evaluate their performance.

- Triangular ramp (TR) test
  The pulse duration rises linearly from 0 to 300 μs and then returns to 0, its range being uniformly distributed.
- Staircase test
  The duration of each pulse changes step by step. The number of steps should be large enough to identify the nonlinearity and their width chosen carefully. Let $\tau = T_s/4$ (where T_s is the 98% settling time). It is then recommended to use mixed step widths, with step width τ for $\frac{1}{3}$ of the test period, 2τ for another $\frac{1}{3}$ of the test period and 3τ for the remaining $\frac{1}{3}$ of the test period, and to randomize these widths when creating the test signals (Zhu, 2000).
- FRN test
  The pulsewidth signal is produced by lowpass filtering white noise, using a suitable cut-off frequency to balance the opposing physiological and identification issues discussed above. Having filtered the signal, an offset and gain are applied to ensure the desired pulsewidth range is spanned.
- PRMS test
  The excitation signal is an multi-level pseudo random signal which is a periodic, deterministic signal having an autocorrelation function similar to white noise. The amplitude level is uniformly distributed over the full range.

6. Results

6.1. Experimental set-up

The ILC workstation has been described in Section 1, and is a platform on which model-based ES has been clinically applied. Experimental tests have been carried out using this system with the objectives of

- providing a facility whose software and hardware components, including sensor and stimulation systems, have been experimentally assessed and verified (Freeman et al., 2009c).
- ensuring that the experimental set-up procedure, as used in clinical trials, is appropriate to the intended application area of stroke rehabilitation.

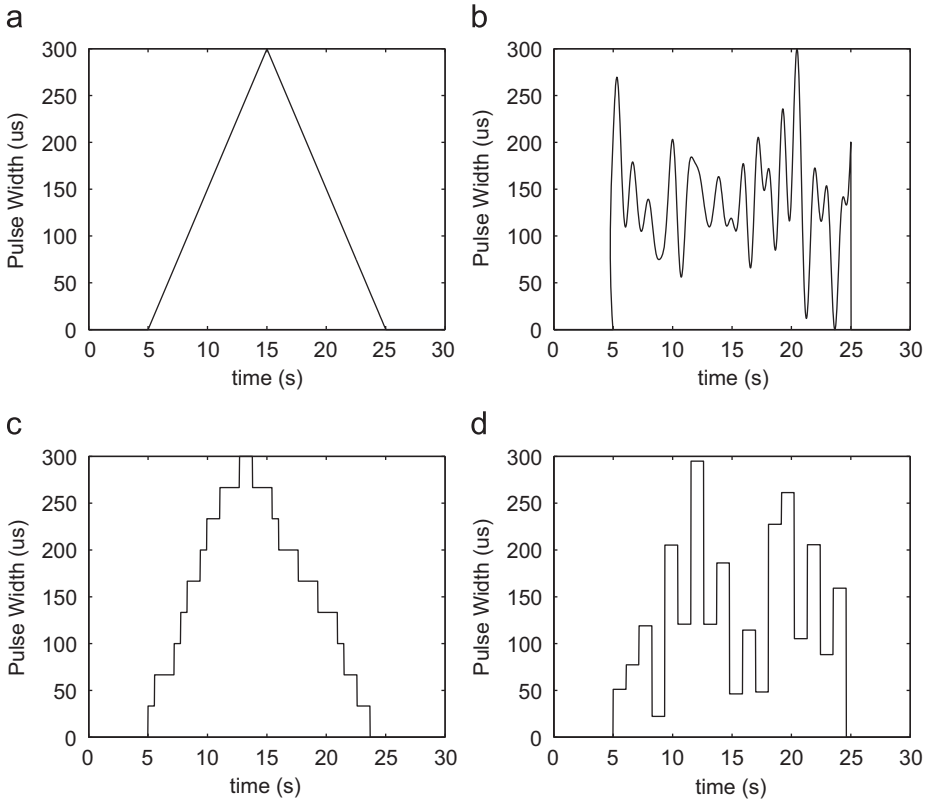

Fig. 5. An example of four candidate tests: (a) triangular ramp test, (b) filtered random noise test, (c) staircase test, and (d) pseudo-random multi-level sequences test.

Tests were performed on a single unimpaired subject, and took place during two sessions conducted over consecutive days. Biometric measurements, including the length of upper arm and forearm, were first made using anatomical landmarks, and then the participant was seated in the workstation. Their right arm was strapped to the extreme link of the five-bar robotic arm which incorporates a six axis force/torque sensor, which provides support and constrains it to lie in a horizontal plane, and straps were also applied about the upper torso to prevent shoulder and trunk movement (as shown in Fig. 1). The subject's upper limb was then moved over as large an area as possible and a kinematic model of the arm was produced using the measurements recorded. This kinematic model is the same as that appearing in the arm and muscle system shown in Fig. 2, but it is now used to convert the force recorded by the force/torque sensor to torque acting about the elbow (full details are given in Freeman et al., 2009c). The electrode was then positioned on the lateral head of triceps and adjusted so that the applied ES generated maximum forearm movement. The stimulation consists of a series of bi-phasic pulses at 40 Hz, whose pulsewidth is variable from 0 to 300 μs with a resolution of 1 μs. The amplitude, which is fixed throughout all subsequent tests, is determined by setting the pulsewidth equal to 300 μs and slowly increasing the applied voltage until a maximum comfortable limit is reached. A sample frequency of 1.6 kHz is used by the real-time hardware, and all calculations are performed using the Matlab/Simulink environment.

The position of the robotic arm was then fixed using a locking pin, at an elbow extension angle of approximately $\pi/2$ rads. This removes the non-isometric components of the biomechanical model, so that the resulting system corresponds to the Hammerstein structure shown in Fig. 3. The identification tests that followed were each of 30 s duration, and used excitation signals in which the first and last 5 s periods consisted of zero stimulation. Only the middle 20 s section of input and output data was used for identification, with the adjoining periods used to establish the baseline torque offset (taken as the mean torque value). The identification calculations were carried out immediately following each test in order to establish the efficacy of the data.

For the TR, Staircase and FRN tests, 10 trials were performed, however, in the case of the PRMS test, only four trials were carried out as it was evident that the fit rate was poor. Between every two tests there was a rest period of at least 10 min in order to eliminate fatigue (Graham, Thrasher, & Popovic, 2006), and the order of identification tests was also randomized to minimize the effect of subject memory or acclimatization increasing the subject's involuntary response.

6.2. Experimental results

For both algorithms, the identification, validation and cross-validation results are listed in Tables 1, 2 and 3, respectively. Results are in terms of the Best Fit rate, defined as the percentage,

$$\text{Best Fit} = \left(1 - \frac{\|y-\hat{y}\|_2}{\|y-\bar{y}\|_2}\right) \times 100$$

where y is the measured output, $\hat{y}$ is the simulated model output and $\bar{y}$ is the mean of y.

Moreover, to aid visual comparison of the identification and validation results between Algorithms 1 and 2, box and whisker plots are presented in Fig. 6.

The identification results for each individual trial of four candidate tests are given together with the average results for all the trials, in Table 1. To obtain the validation results, a model is firstly identified from the data of one trial and then is used to predict the outputs for all the trials in the same type of the tests. The results are the average values of all the prediction results in Best Fit rate. The validation results, in Table 2, show the predictive ability within the same type of identification tests. Similarly, in order to show the predictive ability for different stimulation patterns, cross-validation analysis is conducted, see Table 3. Firstly, a model is identified from the data of all the trials in one type of test and then is used to predict the outputs for all the trials in one of the other tests. The results are again the average value of

Table 1
Identification results of Algorithms 1 and 2 for the four candidate tests.

	Triangular ramp	Filtered random noise	Staircase	PRMS
(a) Algorithm 1				
1	85.88	42.54	87.62	50.34
2	88.34	36.39	89.16	52.48
3	91.33	36.09	85.18	52.43
4	89.23	36.58	89.68	36.69
5	92.25	63.38	89.84	
6	90.68	55.23	91.35	
7	89.14	48.12	88.33	
8	91.41	58.09	88.17	
9	94.25	74.74	83.46	
10	89.02	66.84	91.85	
Average	90.15	51.8	88.46	
(b) Algorithm 2				
1	92.65	73.03	90.89	66.89
2	92.25	65.19	93.32	78.91
3	93.88	51.69	93.49	63.79
4	93.36	70.92	93.49	65.92
5	93.08	79.94	93.77	
6	91.98	68.46	92.34	
7	95.74	58.48	93.38	
8	92.41	61.50	94.66	
9	95.32	79.74	90.85	
10	92.60	71.32	94.23	
Average	93.33	68.03	93.04	68.88

The results are in terms of the Best Fit Rate.

Table 2
Validation results of Algorithms 1 and 2 for the four candidate tests.

	Triangular ramp	Filtered random noise	Staircase	PRMS
(a) Algorithm 1				
1	82.28	28.01	73.99	11.17
2	82.78	45.00	83.63	43.45
3	79.01	40.52	77.77	46.32
4	82.51	8.79	77.27	44.10
5	82.83	37.62	82.72	
6	81.94	28.97	82.28	
7	78.51	40.67	81.20	
8	80.11	30.37	80.68	
9	82.80	44.77	78.09	
10	83.25	−45.65	81.04	
Average	81.60	25.91	79.87	
(b)Algorithm 2				
1	76.12	16.90	75.86	46.08
2	80.94	26.34	84.39	32.15
3	76.58	36.32	83.42	29.50
4	81.80	16.31	83.47	50.22
5	81.79	24.37	75.82	
6	75.98	41.43	83.09	
7	68.03	29.49	83.32	
8	79.87	20.76	81.96	
9	80.32	46.80	80.67	
10	78.61	−30.94	83.81	
Average	78.00	22.78	81.58	39.49

The model is identified from the listed data set and validated on all the data of the same test. The results are the average Best Fit Rate.

the Best Fit rate. Here only the TR, FRN, and Staircase tests are compared, due to the poor performance of the PRMS test in both identification and validation.

7. Discussion

7.1. Initial values for linear parameters

Both algorithms require the initial values of the linear parameters, which can be obtained using any existing method which applies an input suitable for use with stroke patients. One such technique is the ramp deconvolution method (Durfee & MacLean, 1989), which was applied in the ILC stroke rehabilitation project reported in Freeman et al. (2009b), and a representative choice of parameters may be taken. By using this representative estimate as the initial values, both algorithms can both achieve convergence after several iterations, illustrated by Figs. 7(a) and (b). However, irrespective of the iteration number, Algorithm 2 takes a longer period of time because in each iteration, an iterative search is applied.

In order to expedite the identification process of Algorithm 2, a better solution of the linear parameters is required as the initial values. The representative estimate from (Freeman et al., 2009b) is obviously not accurate enough and, moreover, the values of the linear parameters vary widely from subject to subject and it is difficult to find one representative estimate among all the subjects. Therefore, the optimal solution of the linear parameters from Algorithm 1 has been used to initialize Algorithm 2. This thereby united the two algorithms in a single scheme which combines the speed of the first with the accuracy of the second. The results confirm high accuracy with fewer iterations to converge, as illustrated by Fig. 7(c).

Table 3
Cross Validation results of Algorithms 1 and 2 for the TR, FRN, and Staircase tests.

	Triangular ramp (TR)	Filtered random noise (FRN)	Staircase
(a) Algorithm 1			
(TR)	84.83	17.76	47.94
(FRN)	83.96	40.23	71.40
Staircase	79.53	42.67	
(b) Algorithm 2			
(TR)	81.80	41.08	64.11
(FRN)	68.75	46.80	67.86
Staircase	80.72	45.00	84.39

The model is identified from all the data of one type of the test and validated on all the data of the other type of the test. The results are the average Best Fit Rate.

7.2. Algorithms comparison

- Structure and unknown parameters
  A Hammerstein structure is used in both algorithms, while the choice of the linear model is different. Algorithm 1 chooses the ARX linear model, where the white noise is assumed to pass through the denominator dynamics of the linear block before being added to the output. However, it is perhaps not the most natural form from a physical point of view. Thus, another linear model, OE model, is assumed in Algorithm 2, where white noise is added directly to the output, accounting for the measured errors from the equipment. The number of the unknown parameters is kept the same for both algorithms.
- Identification procedure
  The identification procedures of two algorithms are not the same but they both alternatively optimize the nonlinear and linear parameters at each iteration.

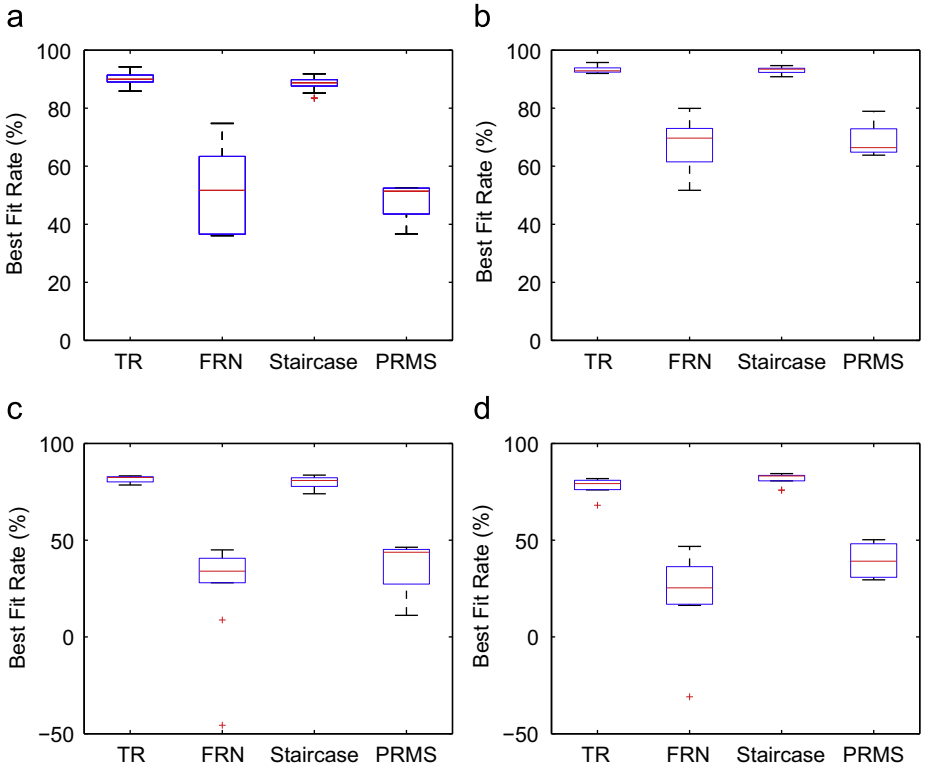

Fig. 6. Comparison between Algorithms 1 and 2 for the identification and validation results: (a) identification results for Algorithm 1, (b) identification results for Algorithm 2, (c) validation results for Algorithm 1, and (d) validation results for Algorithm 2.

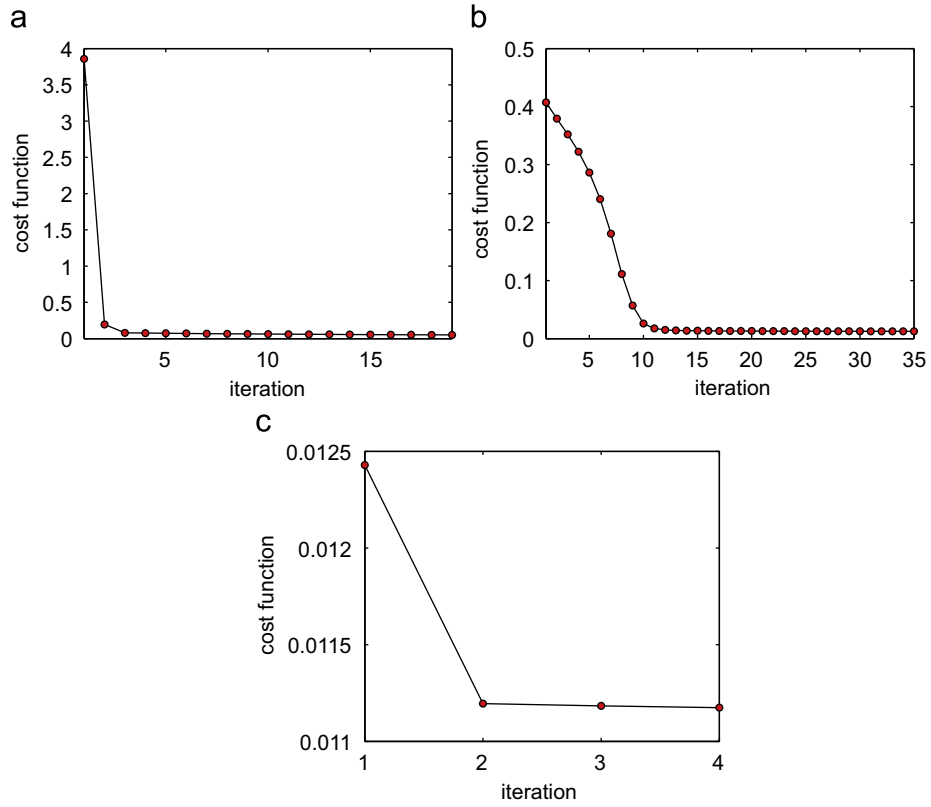

Fig. 7. Examples of convergence properties for Algorithms 1 and 2 are presented: (a) a representative estimate from Freeman et al. (2009b) is used as the initial values and Algorithm 1 is applied. Convergence is achieved after 18 iterations; (b) a representative estimate from Freeman et al. (2009b) is used as the initial values and Algorithm 2 is applied. Convergence is achieved after 35 iterations; and (c) the optimal solution from Algorithm 1 is used to provide the initial values and Algorithm 2 is applied. Convergence is achieved after four iterations.

Algorithm 1 is a development of a two stage identification method, see Le et al. (2009), which has been shown to outperform both the ramp deconvolution and separable least squares methods on a simulated muscle system with a range of noise levels. It alternatively solves the least squares problems to optimize the linear and nonlinear parameters. It is computationally easy and is reasonably fast in implementation.

The identification procedure of Algorithm 2 is more complicated. On each iteration, the nonlinear parameters can be identified through use of transformations and related assumptions, in a least squares sense, while the identification of the linear parameters necessitates an iterative search technique to find the local optimal solution. Thus, it is more time consuming than Algorithm 1, but, by using the optimal solution from Algorithm 1 to provide initial values, the identification procedure of Algorithm 2 can be greatly speeded up to the point where it is not a matter of concern.

- Performance

Both algorithms provide good fitting performance and predictive ability. Fig. 8 shows the fitting performance between the modelled outputs and measured outputs in both identification and validation cases.

In terms of identification results, Algorithm 2 is superior to Algorithm 1, as observed directly from Figs. 6(a) and (b). Numerically, Algorithm 2 improves the average results by up to 20% compared with Algorithm 1, as shown in Table 1.

However, for validation results, both perform similarly, as shown by Figs. 6(c) and (d). Through examination of Table 2, Algorithm 1 is seen to be better for TR and FRN test data, while Algorithm 2 is better for the staircase and PRMS test data. It is therefore reasonable to conclude that both algorithms have comparable performance in prediction.

The validation and prediction results provide the most direct indication of the models' accuracy when applied to the design of controllers for stroke rehabilitation. Since both algorithms exhibit similar performance in this area, it is Algorithm 1's simpler implementation and faster computation that make it the preferable option. Whilst in this application Algorithm 2's increased complexity does not translate to improved results in validation and prediction, it is anticipated that applications exist in which it does outperform Algorithm 1.

7.3. Candidate tests comparison

Although the TR test is widely used in muscle tests such as Freeman et al. (2009b), Durfee and MacLean (1989) and Durfee and Palmer (1994) and can achieve satisfactory fitting rates (almost the highest values in the identification case and approximately 80% for Algorithm 1 and a little lower for Algorithm 2 in the validation case), it shows poor capability in predicting other stimulation patterns, such as those in Table 3. This is due to its non-persistent excitation property discussed in the previous section, which leads to an unreliable model identified from this test.

For the FRN and PRMS tests, the average identification results for Algorithm 1 are 51.8% and 48%, respectively, as shown in Table 1(a). Although Algorithm 2 improves on these by as much as 20%, these tests are still far lower than those of the TR and Staircase tests. The validation results in Table 2 are even lower,

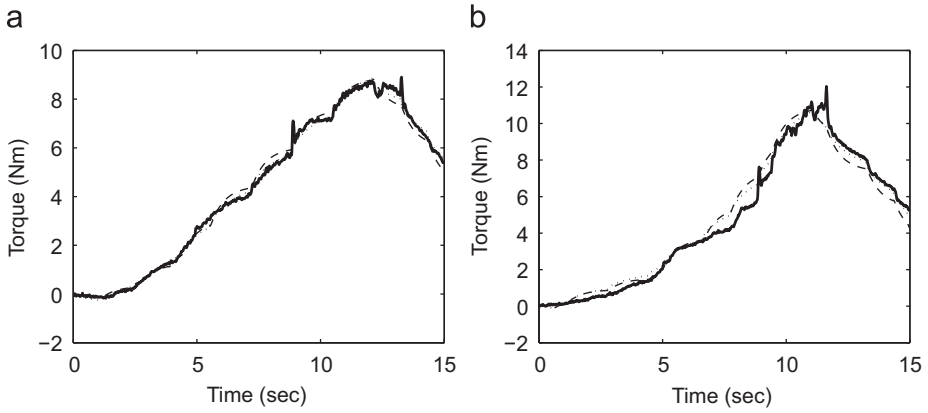

Fig. 8. The force outputs of Algorithm 1 (dashed), Algorithm 2 (dotted) and the measured force outputs (solid) are plotted: (a) identification and (b) validation.

and this lack of output prediction may be expected to lead to poor results when transferred to model-based control application. There may be two reasons for this: the first is that the model structure and the identification algorithms are not proper, but this is not the case because they perform very well for the other two identification tests. The second reason is that the experimental data is not proper. Considering the effects caused by randomly exciting tests on the human subjects, it is believed that these signals elicit involuntary reflexes and subject discomfort, which results in noisy data.

To the best of the authors' knowledge, this is the first time the Staircase test has been used in the identification of electrically stimulated muscles, and it has shown clear advantages over alternatives, i.e. it is persistently exciting, gives high fitting rates in the identification case (the second highest one in Table 1) and in the validation case (surpassing even the TR test for Algorithm 2 in Table 2(b)) and shows accurate predictive ability across different stimulation patterns (see Table 3). Therefore the Staircase test is highly recommended for the identification of electrically stimulated muscle.

8. Conclusion

Two identification schemes have been developed in order to address the limitations in the suitability and effectiveness of existing methods for identification of electrically stimulated muscle models in the case of incomplete paralysis. These limitations relate both to the underlying model structure, and also to the associated excitation input required in the identification of its parameters. Experimental results have been used to confirm the efficacy of each approach and assess their performance over a range of identification test inputs with respect to persistence of excitation and modelling accuracy. Limitations in the identification procedure of each were subsequently overcome by combining them into a unified scheme.

The approach will shortly be applied to stroke participants in clinical trials using the ILC workstation in order to directly verify its capability within upper limb stroke rehabilitation. Based on results presented in this paper, it is anticipated that the increased model accuracy will lead to more precise tracking in a reduced number of trials, thereby increasing the potential of the approach for reduction in impairments.

References

Bai, E. W. (1998). An optimal two-stage identification algorithm for Hammerstein–Wiener nonlinear systems. *Automatica*, *34*(3), 333–338.

Bai, E. W. (2002). A blind approach to the Hammerstein–Wiener model identification. *Automatica*, *38*(6), 967–979.

Bai, E. W., Cai, Z., Dudley-Javorosk, S., & Shields, R. K. (2009). Identification of a modified Wiener–Hammerstein system and its application in electrically stimulated paralyzed skeletal muscle modeling. *Automatica*, *45*(3), 736–743.

Baker, L. L., Wederich, C. L., McNeal, D. R., Newsam, C. J., & Waters, R. L. (2000). Neuromuscular electrical stimulation: A Practical Guide (4th ed.), Los Amigos Research Education Institution Inc.

Baratta, R., & Solomonow, M. (1990). The dynamic response model of nine different skeletal muscles. *IEEE Transactions on Biomedical Engineering*, *37*(3), 243–251.

Bernotas, L., Crago, P. E., & Chizeck, H. J. (1986). A discrete-time model of electrically stimulated muscle. *IEEE Transactions on Biomedical Engineering*, *33*(9), 829–838.

Bobet, J., Gossen, E. R., & Stein, R. B. (2005). A comparison of models of force production during stimulated isometric ankle dorsiflexion in humans. *IEEE Transactions on Neural Systems and Rehabilitation Engineering*, *13*(4), 444–451.

Bobet, J., & Stein, R. B. (1998). A simple model of force generation by skeletal muscle during dynamic isometric contractions. *IEEE Transactions on Biomedical Engineering*, *45*(8), 1010–1016.

Boutayeb, M., Aubry, D., & Darouach, M. (1996). A robust and recursive identification method for MISO Hammerstein model. In UKACC international conference on CONTROL'96 (pp. 234–239).

Braz, G. P., Smith, R. M., & Davis, G. M. (2006). Designing an FES control algorithm: Important considerations. In World Congress on medical physics and biomedical engineering 2006 (pp. 2848–2851), Seoul, Korea.

Broeks, J. G., Lankhorst, G. J., Rumping, K., & Prevo, A. J. (1999). The long-term outcome of arm function after stroke: Results of a follow-up study. *Disability and Rehabilitation*, *21*, 357–364.

Burridge, J. H., & Ladouceur, M. (2001). Clinical and therapeutic applications of neuromuscular stimulation: A review of current use and speculation into future developments. *Neuromodulation*, *4*(4), 147–154.

Carroll, S. G., Triolo, R. J., Chizeck, H. J., Kobetic, R., & Marsolais, E. B. (1989). Tetanic responses of electrically stimulated paralyzed muscle at varying interpulse intervals. *IEEE Transactions on Biomedical Engineering*, *36*(7), 644–653.

Chang, F. H.I., & Luus, R. (1971). A non-iterative method for identification using Hammerstein model. *IEEE Transactions on Automatic Control*, *16*(5), 464–468.

Chizeck, H. J., Chang, S., & Stein, R. B. (1999). Identification of electrically stimulated quadriceps muscles in paraplegic subjects. *IEEE Transactions on Biomedical Engineering*, *46*(1), 51–61.

Chizeck, H. J., Crago, P. E., & Kofman, L. S. (1988). Robust closed-loop control of isometric muscle force using pulsewidth modulation. *IEEE Transactions on Biomedical Engineering*, *35*(7), 510–517.

Chizeck, H. J., Lan, N., Palmieri, L. S., & Crago, P. E. (1991). Feedback control of electrically stimulated muscle using simultaneous pulse width and stimulus period modulation. *IEEE Transactions on Biomedical Engineering*, *38*(12), 1224–1234.

Crago, P. E., Nakai, R. J., & Chizeck, H. J. (1991). Feedback regulation of hand grasp opening and contact force during stimulation of paralysed muscle. *IEEE Transactions on Biomedical Engineering*, *38*(1), 17–28.

Crago, P. E., Peckham, P. H., & Thrope, G. B. (1980). Modulation of muscle force by recruitment during intramuscular stimulation. *IEEE Transactions on Biomedical Engineering*, *27*(12), 679–684.

Davoodi, R., & Andrews, B. J. (1998). Computer simulation of FES standing up in paraplegia: A self-adaptive fuzzy controller with reinforcement learning. *IEEE Transactions on Rehabilitation Engineering*, *6*(2), 151–161.

de Kroon, J. R., & Ijzerman, M. J. (2008). Electrical stimulation of the upper extremity in stroke: Cyclic versus EMG-triggered stimulation. *Clinical Rehabilitation*, *22*, 690–697.

de Kroon, J. R., Ijzerman, M. J., Chae, J., Lankhorst, G. J., & Zilvold, G. (2005). Relation between stimulation characteristics and clinical outcome in studies using electrical stimulation to improve motor control of the upper extremity in stroke. *Journal of Rehabilitation Medicine*, *37*, 65–74.

de Kroon, J. R., van der Lee, J. H., Ijzerman, M. J., & Lankhorst, G. J. (2002). Therapeutic electrical stimulation to improve motor control and functional abilities of the upper extremity after stroke: A systematic review. *Clinical Rehabilitation*, *16*, 350–360.

Dempsey, E. J., & Westwick, D. T. (2004). Identification of Hammerstein models with cubic spline nonlinearities. *IEEE Transactions on Biomedical Engineering*, *51*(2), 237–245.

Ding, J., Wexler, A. S., & Binder-MacLeod, S. A. (2002). A mathematical model that predicts the force–frequency relationship of human skeletal muscle. *Muscle and Nerve*, *26*(4), 477–485.

Durfee, W. K., & MacLean, K. E. (1989). Methods for estimating isometric recruitment curves of electrically stimulated muscle. *IEEE Transactions on Biomedical Engineering*, *36*(7), 654–667.

Durfee, W. K., & Palmer, K. I. (1994). Estimation of force–activation, force–length, and force–velocity properties in isolated, electrically stimulated muscle. *IEEE Transactions on Biomedical Engineering*, *41*(3), 205–216.

Ferrarin, M., Palazzo, F., Riener, R., & Quintern, J. (2001). Model-based control of FES-induced single joint movements. *IEEE Transactions on Neural Systems and Rehabilitation Engineering*, *9*(3), 245–257.

Freeman, C. T., Hughes, A.-M., Burridge, J. H., Chappell, P. H., Lewin, P. L., & Rogers, E. (2009a). Iterative learning control of FES applied to the upper extremity for rehabilitation. *Control Engineering Practice*, *17*(3), 368–381.

Freeman, C. T., Hughes, A.-M., Burridge, J. H., Chappell, P. H., Lewin, P. L., & Rogers, E. (2009b). A model of the upper extremity using surface FES for stroke rehabilitation. *ASME Journal of Biomechanical Engineering*, *131*(1), 031011-1–031011-12.

Freeman, C. T., Hughes, A.-M., Burridge, J. H., Chappell, P. H., Lewin, P. L., & Rogers, E. (2009c). A robotic workstation for stroke rehabilitation of the upper extremity using FES. *Medical Engineering and Physics*, *31*(3), 364–373.

Graham, G. M., Thrasher, T. A., & Popovic, M. R. (2006). The effect of random modulation of functional electrical stimulation parameters on muscle fatigue. *IEEE Transactions on Neural Systems and Rehabilitation Engineering*, *14*(1), 38–45.

Graupe, D., & Kordylewski, H. (1997). Neural network control of neuromuscular stimulation in paraplegics for independent ambulation. In Proceedings of the 19th annual international conference of the IEEE Engineering in Medicine and Biology Society, Chicago, IL (pp. 1088–1091).

Happee, R., & der Helm, F. C.T. V. (1995). The control of shoulder muscles during goal directed movements an inverse dynamic analysis. *Journal of Biomechanics*, *28*(10), 1179–1191.

Hatwell, M. S., Oderkerk, B. J., Sacher, C. A., & Inbar, G. F. (1991). Patient-driven control of FES-supported standing up: A simulation study. *IEEE Transactions on Rehabilitation Engineering*, *36*(6), 683–691.

Hill, A. V. (1938). Then heat of shortening and the dynamic constants of a muscle. *Proceedings of the Royal Society*, *126*, 136–195.

Hughes, A.-M., Freeman, C. T., Burridge, J. H., Chappell, P. H., Lewin, P., & Rogers, E. (2009). Feasibility of iterative learning control mediated by functional electrical stimulation for reaching after stroke. *Journal of Neurorehabilitation and Neural Repair*, *23*(6), 559–568.

Hunt, K. J., Jaime, R. P., & Gollee, H. (2001). Robust control of electrically-stimulated muscle using polynomial H_∞ design. *Control Engineering Practice*, *9*, 313–328.

Hunt, K. J., Munih, M., & Donaldson, N. (1997). Feedback control of unsupported standing in paraplegia—part I: Optimal control approach. *IEEE Transactions on Rehabilitation Engineering*, *5*(4), 331–340.

Hunt, K. J., Munih, M., Donaldson, N., & Barr, F. M.D. (1998). Investigation of the Hammerstein hypothesis in the modeling of electrically stimulated muscle. *IEEE Transactions on Biomedical Engineering*, *45*(8), 998–1009.

Jezernik, S., Wassink, R. G.V., & Keller, T. (2004a). Sliding mode closed-loop control of FES: Controlling the shank movement. *IEEE Transactions on Biomedical Engineering*, *51*(2), 263–272.

Jezernik, S., Wassink, R. G.V., & Keller, T. (2004b). Sliding mode closed-loop control of FES: Controlling the shank movement. *IEEE Transactions on Biomedical Engineering*, *51*(2), 263–272.

Lan, N. (2002). Stability analysis for postural control in a two-joint limb system. *IEEE Transactions on Neural systems and Rehabilitation Engineering*, *10*(4), 249–259.

Lan, N., Feng, H. Q., & Crago, P. E. (1994). Neural network generation of muscle stimulation patterns for control of arm movements. *IEEE Transactions on Rehabilitation Engineering*, *2*(4), 213–224.

Law, L. A.F., & Shields, R. K. (2007). Mathematical models of human paralyzed muscle after long-term training. *Journal of Biomechanics*, *40*, 2587–2595.

Le, F., Markovsky, I., Freeman, C. T., & Rogers, E. (2009). Identification of electrically stimulated muscle after stroke. In European control conference 2009, Budapest, Hungary, (pp. 1576–1581).

Marquardt, D. (1963). An algorithm for least-squares estimation of nonlinear parameters. *SIAM on Journal Applied Mathematics*, *11*, 431–441.

Munih, M., Hunt, K. J., & Donaldson, N. N. (2000). Variation of recruitment nonlinearity and dynamic response of ankle plantarflexoes. *Medical Engineering and Physics*, *22*(2), 97–107.

Narendra, K. S., & Gallman, P. G. (1966). An iterative method for the identification of nonlinear systems using a Hammerstein model. *IEEE Transactions on Automatic Control*, *11*(3), 546–550.

National Audit Office (2005). Reducing brain damage: Faster access to better stroke care. HC 452 2005-2006. URL: ⟨http://www.nao.org.uk⟩.

Parker, V. M., Wade, D. T., & Langton-Hewer, R. (1986). Loss of arm function after stroke: Measurement, frequency and recovery. *International Rehabilitation Medicine*, *8*(2), 69–73.

Popovic, D., & Popovic, M. (1998). Tuning of a nonanalytical hierarchical control system for reaching with FES. *IEEE Transactions on Biomedical Engineering*, *45*(2), 203–212.

Previdi, F., & Carpanzano, E. (2003). Design of a gain scheduling controller for knee-joint angle control by using functional electrical stimulation. *IEEE Transactions on Control Systems Technology*, *11*(3), 310–324.

Previdi, F., Schauer, T., Savaresi, S. M., & Hunt, K. J. (2004). Data-driven control design for neuroprotheses: A virtual reference feedback tuning (VRFT) approach. *IEEE Transactions on Control Systems Technology*, *12*(1), 176–182.

Riener, R., & Fuhr, T. (1998). Patient-driven control of FES-supported standing up: A simulation study. *IEEE Transactions on Rehabilitation Engineering*, *6*(2), 113–124.

Riener, R., & Quintern, J. (1997). A physiologically based model of muscle activation verified by electrical stimulation. *Bioelectrochemistry and Bioenergetics*, *43*, 257–264.

Rushton, D. N. (2003). Functional electrical stimulation and rehabilitation—An hypothesis. *Medical Engineering and Physics*, *25*(1), 75–78.

Schauer, T., Negard, N. O., Previdi, F., Hunt, K. J., Fraser, M. H., & Ferchland, E., et al. (2005). Online identification and nonlinear control of the electrically stimulated quadriceps muscle. *Control Engineering Practice*, *13*, 1207–1219.

Stoica, P. (1981). On the convergence of an iterative algorithm used for Hammerstein system identification. *IEEE Transactions on Automatic Control*, *26*(4), 967–969.

Thorsen, R., Spadone, R., & Ferrarin, M. (2001). A pilot study of myoelectrically controlled FES of upper extremity. *IEEE Transactions on Neural Systems and Rehabilitation Engineering*, *9*(2), 161–168.

Tresadern, P., Thies, S., Kenney, L., Howard, D., & Goulermas, J. Y. (2006). Artificial neural network prediction using accelerometers to control upper limb FES during reaching and grasping following stroke. In Proceedings of the 28th annual international conference of the IEEE Engineering in Medicine and Biology Society (pp. 2916–2919), New York, USA.

Veltink, P. H., Chizeck, H. J., Crago, P. E., & El-Bialy, A. (1992). Nonlinear joint angle control for artificially stimulated muscle. *IEEE Transactions on Biomedical Engineering*, *39*(4), 368–380.

Watanabe, T., Iibuchi, K., Kurosawa, K., & Hoshimiya, N. (2003). A method of multichannel PID control of two-degree-of-freedom wrist joint movements by functional electrical stimulation. *Systems and Computers in Japan*, *34*(5), 319–328.

Westwick, D. T., & Kearney, R. E. (2001). Separable least squares identification of nonlinear Hammerstein models: Application to stretch reflex dynamics. *Annals of Biomedical Engineering*, *29*(8), 707–718.

Zhu, Y. (2000). Identification of Hammerstein models for control using ASYM. *International Journal of Control*, *73*(18), 1692–1702.